

Shear-forced vertical circulations in tropical cyclones

Da-Lin Zhang and Chanh Q. Kieu

Department of Atmospheric and Oceanic Science, University of Maryland, College Park, Maryland, USA

Received 4 April 2005; revised 6 June 2005; accepted 13 June 2005; published 15 July 2005.

[1] The forced secondary circulation (FSC) by the vertical shear of horizontal winds is isolated from the latent heating and friction FSCs associated with a model-simulated hurricane vortex. This is achieved by use of a newly developed potential vorticity inversion and quasi-balanced vertical motion equations system. Results show that latent heating forces intense updrafts in the eyewall and slow subsidence in the eye, whereas the friction-FSC is similar to that of the Ekman pumping, with the peak ascent occurring near the top of the boundary layer in the eye. In contrast, when an environmental westerly shear is superposed with an axisymmetric balanced vortex, an anticlockwise FSC appears across the inner-core region with the rising motion downshear and easterly sheared horizontal flows in the vertical. The resulting horizontal flows act to reduce the influence of the vertical shear inside the storm by as much as 30–40%, thus opposing the destructive roles of the vertical shear. **Citation:** Zhang, D.-L., and C. Q. Kieu (2005), Shear-forced vertical circulations in tropical cyclones, *Geophys. Res. Lett.*, *32*, L13822, doi:10.1029/2005GL023146.

1. Introduction

[2] It is well known that a tropical-cyclone (TC) vortex in a sheared environment has upward motion on its downshear side [Raymond, 1992; Jones, 1995]. Such a vertical motion asymmetry arises from the storm-relative movement of air parcels up and down the deformed isentropic surfaces that are lowered (raised) on the up- (down-) shear side of the warm-cored vortex. The TC vortex also tends to tilt downshear, partly accounting for the observed decrease in the storm intensity [Gray, 1968; DeMaria, 1996; Black *et al.*, 2002]. A warm-core anomaly is required in order for the vortex to remain in thermal-wind balance. The vertical motion asymmetry and the downshear tilt have been confirmed by idealized, three-dimensional (3D) numerical simulations of TC-like vortices [e.g., Wang and Holland, 1996; Frank and Ritchie, 1999, 2001], and recent real-data simulations of hurricanes (e.g., Bonnie (1998)) under the influence of intense shear [see Rogers *et al.*, 2003; Zhu *et al.*, 2004].

[3] Because of its importance in determining the TC structures and intensity, considerable attention has recently been paid to various effects of vertical shear and the dynamics of the vertical motion asymmetry [Jones, 1995, 2004; Zhu *et al.*, 2004; Wang *et al.*, 2004]. However, few studies have been performed to isolate the shear-forced secondary circulation (FSC) from the total FSCs and investigate the impact of the shear-FSC on the dynamics of TCs and other cyclonic vortices, except for sensitivity studies.

Thus, in this study, we attempt to address the above issue by separating the FSCs by the dry dynamical, latent heating and planetary boundary layer (PBL) processes using a recently developed potential vorticity (PV) inversion and quasi-balanced vertical motion ω equations (PV- ω) system by Wang and Zhang [2003], hereafter referred to as WZ.

[4] The next section describes briefly the methodology used to separate the FSCs by the above-mentioned processes. Section 3 presents their different characteristics, and shows the effects of removing the vertical shear. Section 4 provides a summary and concluding remarks on the relationship between the shear- and the total-FSCs, with a revised explanation of the effects of vertical shear on the dynamics of TCs.

2. Methodology

[5] In the PV- ω system, the stream function ψ and geopotential height ϕ fields are first obtained by inverting the nonlinear balance and PV equations for a given PV field, and then a closed set of quasi-balanced ω equations is solved to yield the FSCs by various physical and dynamical processes. The ω -equation in the vertical, pseudo-height z -coordinates is given by

$$\begin{aligned} \nabla^2 \left(\frac{\partial^2 \phi}{\partial z^2} \omega \right) + f \eta \frac{\partial}{\partial z} \left\{ (z_a - z)^{-\mu} \frac{\partial}{\partial z} [(z_a - z)^\mu \omega] \right\} \\ - f \frac{\partial}{\partial z} \left(\frac{\partial \omega}{\partial x} \frac{\partial^2 \psi}{\partial x \partial z} + \frac{\partial \omega}{\partial y} \frac{\partial^2 \psi}{\partial y \partial z} \right) \\ - f \frac{\partial}{\partial z} \left(\frac{\partial \omega}{\partial x} \frac{\partial^2 \chi}{\partial y \partial z} - \frac{\partial \omega}{\partial y} \frac{\partial^2 \chi}{\partial x \partial z} \right) \\ - \left(f \frac{\partial \eta}{\partial z} \frac{\mu}{z_a - z} + f \frac{\partial^2 \eta}{\partial z^2} \right) \omega \\ = f \frac{\partial}{\partial z} [\mathbf{V}_h \cdot \nabla \eta] - \nabla^2 \left[\mathbf{V}_h \cdot \nabla \frac{\partial \phi}{\partial z} \right] \\ - \beta \frac{\partial^3 \psi}{\partial t \partial y \partial z} - 2 \frac{\partial^2}{\partial t \partial z} J \left(\frac{\partial \psi}{\partial x}, \frac{\partial \psi}{\partial y} \right) + \frac{g}{\theta_0} \nabla^2 \dot{q} \\ - f \frac{\partial}{\partial z} \left(\frac{\partial f_y}{\partial x} - \frac{\partial f_x}{\partial y} \right) - \frac{\partial^2}{\partial t \partial z} \left(\frac{\partial f_x}{\partial x} + \frac{\partial f_y}{\partial y} \right) \end{aligned} \quad (1)$$

where ∇ is a horizontal gradient operator, $\mu = C_p/R_d$ and $z_a = C_p \theta_0/g$; $\eta = \zeta + f$; χ is the velocity potential; $\mathbf{V}_h = \mathbf{V}_\psi + \mathbf{V}_\chi$ is the horizontal velocity including the balanced (\mathbf{V}_ψ) and divergent (\mathbf{V}_χ) components; \dot{q} is the latent heating rate; f_x and f_y denote the frictional processes mainly due to the PBL plus small numerical diffusion effects along the x - and y - axes, respectively; and all the other variables assume their typical meteorological meaning. The vertical motion ω can be inverted from equation (1), given its right-hand side (RHS) terms that, from the left to right, are the differential absolute vorticity advection and the Laplacians of thermal

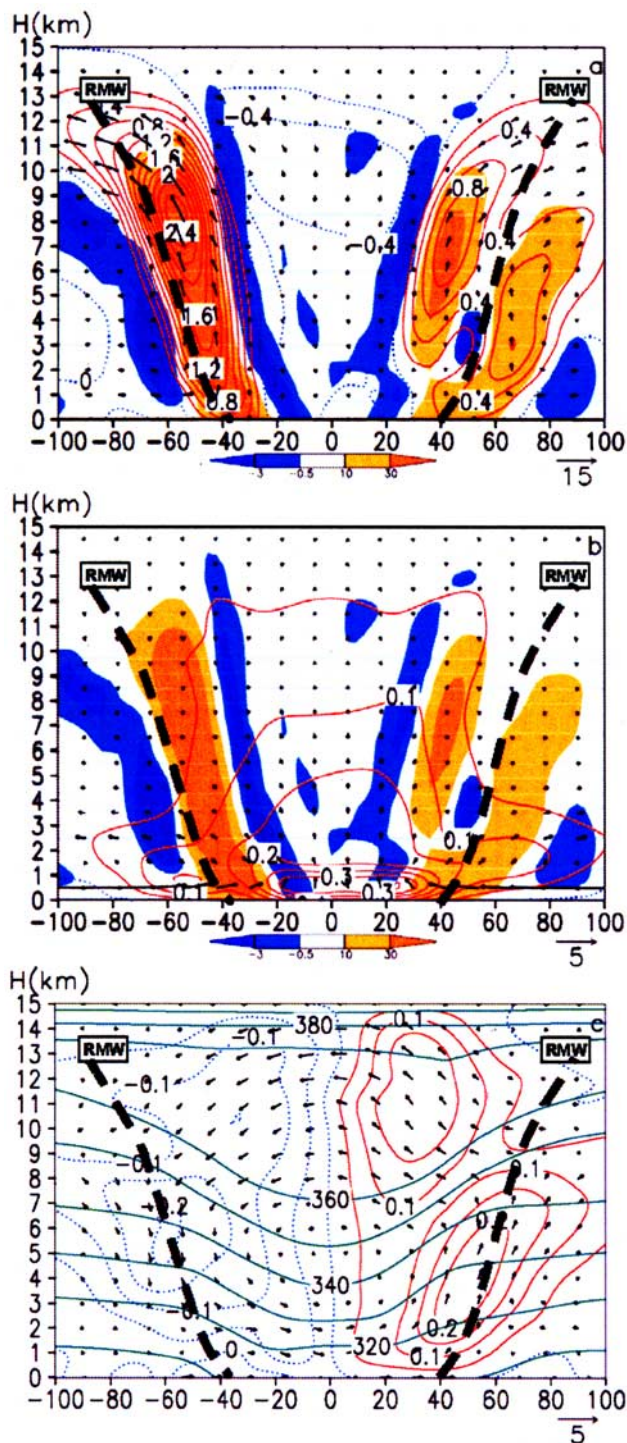


Figure 1. West-east vertical cross sections through the storm center of (storm-relative) in-plane flow vectors and the vertical motion forced by (a) latent heating (every 0.2 m s^{-1}); (b) the PBL (every 0.05 m s^{-1}); and (c) the dry dynamical processes (every 0.05 m s^{-1}), which are obtained from the 56–57 h simulation ending 2100 UTC 23 August 1992. Shadings denote the latent heating (orange) or cooling (blue) rates in K h^{-1} . Solid (dotted) lines are for upward (downward) motion, and green lines in Figure 1c are isentropes. Note that the vertical motion vectors have been amplified by a factor of 5.

advection by both nondivergent and divergent winds, the β effect, the Jacobian term, latent heating rates, and the PBL effects, respectively. The first four RHS terms are considered herein as the dry-dynamical processes and they are of our major concern for the present study.

[6] Because of the existence of local tendency terms, equation (1) is not a fully diagnostic equation. Thus, the frictional terms of $\partial f_x/\partial t$ and $\partial f_y/\partial t$ (as well as latent heating rates) are directly from the model output; the terms containing $\partial\psi/\partial t$ are obtained by solving the vertical vorticity ζ equation; and the velocity potential χ is related to ω through the continuity equation. Solving a closed set of equations in ω , χ and $\partial\psi/\partial t$ yields the vertical motion ω and divergent flows V_χ or FSCs (see section 3 in WZ for a detailed description of computational procedures). A cloud-resolving simulation of Hurricane Andrew (1992) with the finest grid size of 6 km [see Liu *et al.*, 1997], which is the same as that used by WZ, is utilized for the present study.

3. Results

[7] Because equation (1) is an elliptic equation, the FSCs by the individual processes can be separately inverted after obtaining the balanced ψ and ϕ fields. Figures 1a–1c show the west-east cross sections of the FSCs by the latent heating, PBL and dry dynamical processes, respectively. The latent heating FSC exhibits a typical vertical circulation of TCs with the bottom-inward, midlevel slantwise and upper-level outward flows. As expected, the distribution of intense updrafts coincides with that of latent heat release in the eyewall and outer rainbands. The slantwise updrafts follow closely moist-isentropic surfaces in the eyewall [see Zhang *et al.*, 2002]. Of relevance to this study is that the latent heat release in the eyewall induces weak compensating subsidence from the tropopause to the surface in the eye, with stronger subsidence occurring aloft.

[8] The PBL processes produce radial inflows in the bottom layers that begin to ascend in the eyewall and reach a peak value as large as 0.3 m s^{-1} near the top of the PBL at the circulation center in the eye (Figure 1b). This ascending motion, decreasing upward, could reach the upper outflow layer to offset some portion of the eye subsidence induced by latent heating in the eyewall (see Figures 1a and 1b). Apparently, the PBL-FSC is similar to that by the Ekman pumping leading to the spin-down of a cyclonic vortex [Holton, 2004].

[9] In contrast, the FSC by the dry dynamical processes is a deep anticlockwise circulation across the storm with a rising (descending) motion in the eastern (western) portion of the eyewall, and an easterly (westerly) flow across the eye aloft (below) (Figure 1c). Note that this FSC contains two vertical motion couplets that appear to be closely related to the abrupt shift in the environmental vertical shear and the changes in vortex structure within the radius of maximum wind (RMW). Such wave number-1 vertical motion couplets also appear in the horizontal plane, but with the updraft core shifted from the east-southeast at $H = 4 \text{ km}$ to south-southeast at $H = 10 \text{ km}$ in the eyewall (not shown). Note also that the vertical axis of the eye center, coinciding roughly with the vertical trough axis of isentropic surfaces, demarcates closely the ascending and descending motions.

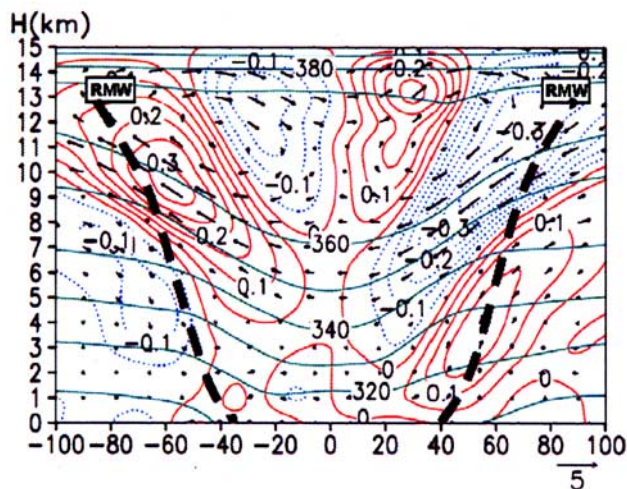


Figure 2. As in Figure 1c, but for the FSC after removing the environmental vertical shear.

[10] The above wave number-1 vertical motion structure in the eyewall appears to be similar to the typical impact of a westerly shear on the asymmetry of clouds/precipitation in TCs. An examination of the RHS terms of equation (1) shows that the dry dynamical processes are determined by the Laplacians of thermal advection, the Jacobian term, the vertical differential vorticity advection and the β term, in that order (not shown). Like in the quasi-geostrophic ω equation, some cancellation occurs between the Laplacians of thermal advection and the vertical differential vorticity advection [Holton, 2004]. As pointed out by Walters [2001], because they are not Galilean invariant, these two terms do not have physical significance in forcing the vertical motion when considered separately. Trenberth [1978] showed that the two terms could be combined into one term involving the dot product of vertical shear and geostrophic vorticity gradient. This implies that vertical motion in the quasi-geostrophic framework will vanish in the absence of vertical shear. It can be easily shown that a similar but slight complicated relationship between the quasi-gradient-balanced vertical motion and the vertical shear (or mean flow) can be derived for the first four terms on the RHS of equation (1). Based on the above analysis, we may hypothesize that the deep anticlockwise vertical circulation shown in Figure 1c is mainly forced by the vertical wind shear in the environment and at the storm scale.

[11] The following steps are taken to validate the above hypothesis. First, an area-averaged vertical (storm-relative) profile of horizontal velocity is obtained over an area of $576 \text{ km} \times 576 \text{ km}$ centered in the eye. This profile should represent roughly the vertical distribution of the environmental winds. The associated hodograph exhibits markedly varying shear vectors in the four major layers with a thickness of 200–300 hPa (not shown). Second, the mean vertical shears in all the layers are subtracted from the original data set, and the resulting PV field is then inverted to yield a new set of the balanced ψ and ϕ fields. Finally, a closed set of equations in ω , χ and $\partial\psi/\partial t$ is iteratively solved to obtain the dry-dynamics FSC.

[12] The result is given in Figure 2, which shows marked changes in the structures and magnitudes of the FSC after

removing the environmental shear. That is, this FSC is much shallower, albeit stronger in intensity, than the original case. In particular, it becomes clockwise with a reversed vertical motion couplet (see Figures 1c and 2). This reversed FSC could be attributed to the presence of negative vertical shear in the eyewall interacting with the mean flow associated with the storm movement.

[13] Because of the complicated vertical shear structures and vortex asymmetry, it is not possible to attribute the shear-FSCs in the original and the shear-removal cases to any layer of vertical shear (see Figures 1c and 2). To help gain insight into the shear-FSC, we use an axisymmetric balanced vortex with no mean flow that is obtained by azimuthally averaging the balanced control vortex. Then, a constant westerly shear of 10^{-3} s^{-1} with a vanishing surface flow is superimposed to the vortex throughout the model atmosphere. The shear-FSC is inverted from the new PV field following the same steps as mentioned above. This should be the “cleanest” validation of the above-mentioned hypothesis. The result is given in Figure 3, which shows that the shear-FSC in this “idealized” case is similar in structure and intensity to that shown in Figure 1c, except that it is more limited within the RMW. It follows that it is the interaction of the hurricane vortex with the environmental vertical shear that accounts for the above-mentioned deep anticlockwise FSC. Apparently, it is this forced vertical motion asymmetry that is mostly responsible for the observed wave number-1 structure of clouds and precipitation in TCs.

[14] Of importance is that the horizontal component of this FSC, which is just a consequence of the mass continuity associated with the vertical motion couplet, acts to reduce the vertical shear within the core region. In the present case, a vertical shear of 10^{-3} s^{-1} could force a vertical motion couplet of $\pm 0.3 \text{ m s}^{-1}$, and the horizontal across-storm flows of $\pm 1.5\text{--}2.5 \text{ m s}^{-1}$ in the eye that are faster than the system-relative flow at the low levels but about 1/4 of the environmental flow aloft (Figure 3). This implies that the FSC could reduce 30–40% of the destruction by vertical shear, thereby helping restore the quasi-balanced properties

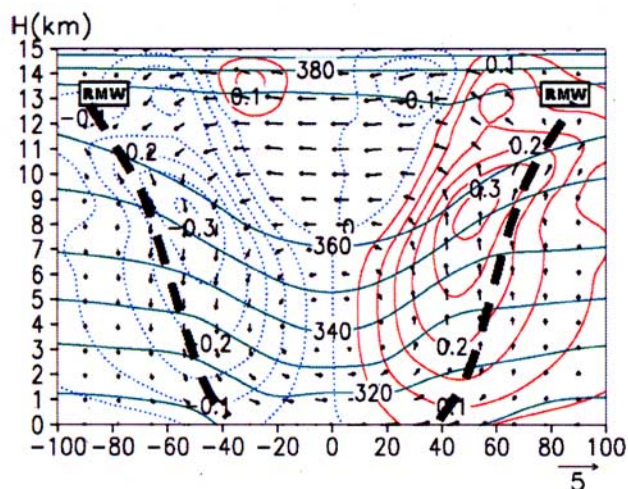


Figure 3. As in Figure 1c, but for the FSC by a westerly shear of 10^{-3} s^{-1} associated with an axisymmetric balanced vortex.

of the vortex. Jones [1995] and Wang and Holland [1996] found similar divergent horizontal flows at the lowest model layer in their idealized simulations of the respective dry barotropic and moist baroclinic vortices with primitive equations models, even under weaker ($\sim 0.4 \times 10^{-3} \text{ s}^{-1}$) sheared environments. However, the divergent flow magnitude obtained by Wang and Holland is about 10 m s^{-1} that is much greater than the present one ($\sim 1.5 \text{ m s}^{-1}$) due partly to the use of different diagnostic approaches, and partly to the implicitly included latent heating effects.

4. Concluding Remarks

[15] In this study, we have used our newly developed PV- ω (elliptic) equations system as a tool to separate the shear-FSC from the latent heating and PBL FSCs associated with a simulated 3D hurricane. It is shown that latent heating accounts for most of upward mass fluxes in the eyewall, and subsidence in the eye. The friction-FSC is similar to that of the Ekman pumping with its peak upward motion occurring near the top of the PBL in the eye. In contrast, the dry dynamical processes, dominated by the environmental vertical shear (and mean flows), produce an anticlockwise FSC in the inner-core region with the rising motion downshear and the sheared horizontal flows opposing the mean shear vector.

[16] It is important to note that the shear-FSC presented herein is contradictory to the traditional view that the inner-core (storm-relative) flows increase with height in the same manner as the environmental flows. Our findings from the FSCs by various processes appear to offer some new understanding of the impact of vertical shear on the dynamics of TCs and other types of cyclonic vortices. First, while vertical shear is inimical to the TC development, the shear-FSC acts to reduce the destructive effects of the shear and resist the downshear tilt of a TC vortex, as also indicated by Jones [1995] and Wang and Holland [1996], thereby helping restore the vortex's properties. This appears to explain to a certain extent why some intense TCs can resist vertical shear as large as $1.5 \times 10^{-3} \text{ s}^{-1}$ [Rogers et al., 2003; Zhu et al., 2004; Wang et al., 2004], and why the inner core of a dry vortex could remain upright while its outer portion is markedly tilted [Jones, 1995, 2004]. Second, the shear-FSC tends to reduce the low-level inflow and upper-level outflow on the downshear side but enhance them on the upshear side, with little impact in the mid-troposphere. This would reduce the downshear advection of warm air from the eye region. The vortex-restoring effects also explain partly why some portion of environmental air is forced to flow, more in the upper troposphere, around a TC, making it move with the mean flow more like an "obstacle." Third, for any moist, warm-cored vortex in a sheared environment, we should expect several physical and dry dynamical processes that are all operative during the life cycle. It should be the total FSC that follows isentropic surfaces in dry stratifications, and moist-isentropic surfaces in saturated stratifications. Evidently, the previous postulation that the vertical shear tends to force air motion along isentropic surfaces should be revised in the context of the present work, even in the warm-core region of TCs. Nevertheless, the shear-induced vertical motion asymmetry appears to be qualitatively consistent with the sloping

isentropes as discussed by previous researchers [Raymond, 1992; Jones, 1995], which can also be seen from Figures 1c, 2, and 3.

[17] Finally, it should be mentioned that the present storm does not exhibit significant downshear tilt. This is partly because the environmental shear associated with Hurricane Andrew (1998) is relatively weak, and partly because intense latent heat release in the eyewall during its rapid deepening stage tends to oppose the forced tilting by the vertical shear by coupling the lower to upper-level vortex flows. In addition, the shear-FSC must have also played a role in resisting the downshear tilt of the storm. A detailed analysis of the effects of vertical shear on the vertical motion asymmetry and circulation characteristics will be presented in a forthcoming journal article.

[18] **Acknowledgments.** We wish to thank Xingbao Wang for his programming assistance, and two anonymous reviewers for their helpful comments. This work was supported by NSF grants ATM-9802391 and ATM-0342363, NASA grant NAG-57842, and ONR grant N00014-96-1-0746.

References

- Black, M. L., J. F. Gamache, F. D. Marks Jr., C. E. Samsury, and H. E. Willoughby (2002), Eastern Pacific Hurricanes Jimena of 1991 and Olivia of 1994: The effect of vertical shear on structure and intensity, *Mon. Weather Rev.*, *130*, 2291–2312.
- DeMaria, M. (1996), The effect of vertical shear on tropical cyclone intensity change, *J. Atmos. Sci.*, *53*, 2076–2087.
- Frank, W. M., and E. A. Ritchie (1999), Effects of environmental flow upon tropical cyclone structure, *Mon. Weather Rev.*, *127*, 2044–2061.
- Frank, W. M., and E. A. Ritchie (2001), Effects of vertical wind shear on the intensity and structure of numerically simulated hurricanes, *Mon. Weather Rev.*, *129*, 2249–2269.
- Gray, W. M. (1968), Global view of the origin of tropical disturbances and storms, *Mon. Weather Rev.*, *96*, 669–700.
- Holton, J. R. (2004), *An Introduction to Dynamic Meteorology*, 4th ed., 535 pp., Elsevier, New York.
- Jones, S. C. (1995), The evolution of vortices in vertical shear: Part I. Initially barotropic vortices, *Q. J. R. Meteorol. Soc.*, *121*, 821–851.
- Jones, S. C. (2004), On the ability of dry tropical-cyclone-like vortices to withstand vertical shear, *J. Atmos. Sci.*, *61*, 114–119.
- Liu, Y., D.-L. Zhang, and M. K. Yau (1997), A multiscale numerical study of Hurricane Andrew (1992): Part I. An explicit simulation, *Mon. Weather Rev.*, *125*, 3073–3093.
- Raymond, D. J. (1992), Nonlinear balance and potential-vorticity thinking at large Rossby number, *Q. J. R. Meteorol. Soc.*, *118*, 987–1015.
- Rogers, R. F., S. S. Chen, J. E. Tenerelli, and H. Willoughby (2003), A numerical study of the impact of vertical shear on the distribution of rainfall in Hurricane Bonnie (1998), *Mon. Weather Rev.*, *131*, 1577–1599.
- Trenberth, K. E. (1978), On the interpretation of the diagnostic quasi-geostrophic omega equation, *Mon. Weather Rev.*, *106*, 131–137.
- Walters, M. K. (2001), A simple example of Galilean invariance in the omega equation, *Bull. Am. Meteorol. Soc.*, *82*, 463–472.
- Wang, X., and D.-L. Zhang (2003), Potential vorticity diagnosis of a simulated hurricane: Part I. Formulation and quasi-balanced flow, *J. Atmos. Sci.*, *60*, 1593–1607.
- Wang, Y., and G. J. Holland (1996), Tropical cyclone motion and evolution in vertical shear, *J. Atmos. Sci.*, *53*, 3313–3332.
- Wang, Y., M. T. Montgomery, and B. Wang (2004), How much vertical shear can a tropical cyclone resist?, *Bull. Am. Meteorol. Soc.*, *85*, 661–662.
- Zhang, D.-L., Y. Liu, and M. K. Yau (2002), A multiscale numerical study of Hurricane Andrew (1992): Part V. Inner-core thermodynamics, *Mon. Weather Rev.*, *130*, 2745–2763.
- Zhu, T., D.-L. Zhang, and F. Weng (2004), Numerical simulation of Hurricane Bonnie (1998): Part I. Eyewall evolution and intensity changes, *Mon. Weather Rev.*, *132*, 225–241.

C. Q. Kieu and D.-L. Zhang, Department of Atmospheric and Oceanic Science, University of Maryland, College Park, MD 20742, USA. (dalin@atmos.umd.edu)